



## New findings of cyclohexane-fused octahydroquinolizine alkaloids from *Myrioneuron faberi*



Ming-Ming Cao<sup>a,b</sup>, Jia-Hui Zhang<sup>b</sup>, Yu Zhang<sup>b</sup>, Zong-Gen Peng<sup>c</sup>, Jian-Dong Jiang<sup>c</sup>, Xiao-Jiang Hao<sup>b,\*</sup>

<sup>a</sup> College of Food Science and Technology, Nanjing Agricultural University, Nanjing 210095, Jiangsu, People's Republic of China

<sup>b</sup> State Key Laboratory of Phytochemistry and Plant Resources in West China, Kunming Institute of Botany, Chinese Academy of Sciences, Kunming 650201, Yunnan, People's Republic of China

<sup>c</sup> Institute of Medicinal Biotechnology, Chinese Academy of Medical Sciences and Peking Union Medical College, Beijing 100050, People's Republic of China

### ARTICLE INFO

#### Article history:

Received 20 September 2016

Revised 27 October 2016

Accepted 1 November 2016

Available online 2 November 2016

#### Keywords:

Myrioneuron alkaloids

Hemiacetal epimers

Lysine-based origination

### ABSTRACT

Cyclohexane-fused octahydroquinolizine (COHQ) alkaloids present an unwonted carbon framework among alkaloids isolated from genus *Myrioneuron*, which featured with bridge-ring and hemiacetal groups. Continued chemical investigation of *Myrioneuron faberi* led to the isolation of four COHQ related structures,  $\beta$ -myrifabral C (**1**),  $\alpha$ -myrifabral C (**2**),  $\beta$ -myrifabral D (**3**), and  $\alpha$ -myrifabral D (**4**). **1** and **2** were inseparable hemiacetal epimers (cluster A), as did **3** and **4** (cluster B). The structures of **1–4** were elucidated on basis of MS and NMR spectra. In vitro, cluster A showed moderate inhibition activity against hepatitis C virus (HCV) replication with therapeutic index (CC<sub>50</sub>/EC<sub>50</sub>) of 74.0.

© 2016 Elsevier Ltd. All rights reserved.

*Myrioneuron* alkaloids are a class of fast growing natural products elaborated by plants of the genus *Myrioneuron*. The lysine-based origination of *Myrioneuron* alkaloids was suggested,<sup>1–3</sup> and the reactive C<sub>5</sub> units derived from lysine constructed intricate polycyclic ring systems (tri-, tetra-, penta-, hexa-, and decacyclic types).<sup>4–10</sup> A number of these structural distinctive alkaloids exhibited antimalarial,<sup>2</sup> antimicrobial,<sup>7</sup> and anti-HCV activities,<sup>7–11</sup> and attracted great organic synthesis interests.<sup>1,2,12–15</sup> Recent phytochemical investigation of *M. faberi*, *M. effusum*, and *M. tonkinensis* resulted in several interesting carbon frameworks,<sup>7–11,16–18</sup> which bring new insights into the biogenetical pathway and structural diversity of *Myrioneuron* alkaloids.

Cyclohexane-fused octahydroquinolizine (COHQ) alkaloids are a group of metabolites obtained from *M. faberi*.<sup>8</sup> Its unique octahydroquinolizine (OHQ) core was differed from other *Myrioneuron* alkaloids, and also featured with a bridge-ring and a hemiacetal groups. However, COHQ alkaloids show no exception with other typical *Myrioneuron* alkaloids, they all holding 'n × C<sub>5</sub>' carbon frameworks (C<sub>10</sub>, C<sub>15</sub>, C<sub>20</sub>, and C<sub>35</sub>).<sup>3,7</sup>

During our ongoing investigation of structurally unique and biologically interesting *Myrioneuron* alkaloids, two C<sub>20</sub> COHQ structures (**1** and **2**) and two C<sub>15</sub> ones (**3** and **4**) were obtained. **1** and **2** presented a new carbon skeleton bearing a '–(CH<sub>2</sub>)<sub>5</sub>–' straight

chain attached to the previously reported C<sub>15</sub> COHQ carbon framework (myrifabral A)<sup>8</sup> through carbon-carbon bond. **3** and **4** presented C-6 epimer of myrifabral A. These findings to some degree broadened our understanding of structural diversity of *Myrioneuron* alkaloids. In this work, we report the isolation, structure elucidation, bioactivity, and hypothesized biogenetical pathway of **1–4**.

Cluster A (**1** and **2**)<sup>19</sup> was obtained as colorless gum. The NMR spectrum of Cluster A exhibited a mixture of two compounds' resonance signals (S1.1–1.6 in Supporting Information), and the downfield '–CH–' signals ( $\delta_{C-13} = 98.2$  and  $\delta_{C-12} = 80.7$  in **1**;  $\delta_{C-13} = 92.2$  and  $\delta_{C-12} = 72.6$  in **2**) (Tables 1 and 2) suggested it to be a pair of hemiacetal epimers as myrifabral A.<sup>8</sup> Because **1** and **2** are isomers, their molecular formula C<sub>20</sub>H<sub>35</sub>NO<sub>3</sub> was revealed by HRESIMS data (*m/z* found 337.2635 for [M]<sup>+</sup>; calcd. for C<sub>20</sub>H<sub>35</sub>NO<sub>3</sub>, 337.2617). The molecular formula C<sub>20</sub>H<sub>35</sub>NO<sub>3</sub> indicated that **1** and **2** possessing four devices of hydrogen deficiency. The <sup>13</sup>C NMR, DEPT and HSQC spectra of the mixture of **1** and **2** (S1.2 and S1.4 in Supporting Information) revealed that there are 40 carbon signals comprising 2 × (14 × CH<sub>2</sub>, 5 × CH, 1 × qC) carbon atoms (Fig. 1). In addition, the typical nitrogenated carbon atoms in COHQ alkaloids (C-2, C-6, and C-16, see Table 1), and highfield quaternary carbon atoms ( $\delta_{C-11} = 32.1$  in **1**;  $\delta_{C-11} = 32.6$  in **2**) were observed. The above featured NMR data and the four devices of hydrogen deficiency indicated **1** and **2** possessed the COHQ carbon framework.

\* Corresponding author.

E-mail address: [haoxj@mail.kib.ac.cn](mailto:haoxj@mail.kib.ac.cn) (X.-J. Hao).

**Table 1**  
<sup>13</sup>C NMR data for **1–4** ( $\delta$  in ppm).

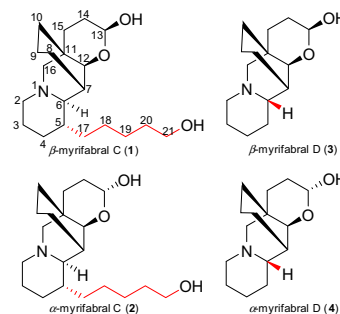
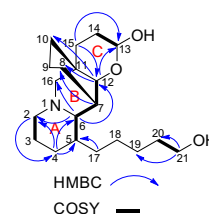
No.	<b>1</b> <sup>a</sup>	<b>2</b> <sup>a</sup>	<b>3</b> <sup>b</sup>	<b>4</b> <sup>b</sup>
2	57.1 (CH <sub>2</sub> )	57.1 (CH <sub>2</sub> )	54.8 (CH <sub>2</sub> )	54.7 (CH <sub>2</sub> )
3	26.4 (CH <sub>2</sub> )	26.4 (CH <sub>2</sub> )	25.9 (CH <sub>2</sub> )	26.1 (CH <sub>2</sub> )
4	30.4 (CH <sub>2</sub> )	30.4 (CH <sub>2</sub> )	22.6 (CH <sub>2</sub> )	22.5 (CH <sub>2</sub> )
5	37.2 (CH)	37.3 (CH)	29.8 (CH <sub>2</sub> )	29.9 (CH <sub>2</sub> )
6	70.3 (CH)	70.8 (CH)	64.1 (CH)	64.5 (CH)
7	35.3 (CH)	35.0 (CH)	40.2 (CH)	40.0 (CH)
8	20.7 (CH <sub>2</sub> )	20.5 (CH <sub>2</sub> )	19.2 (CH <sub>2</sub> )	19.4 (CH <sub>2</sub> )
9	21.4 (CH <sub>2</sub> )	21.5 (CH <sub>2</sub> )	25.4 (CH <sub>2</sub> )	25.4 (CH <sub>2</sub> )
10	29.5 (CH <sub>2</sub> )	28.6 (CH <sub>2</sub> )	29.2 (CH <sub>2</sub> )	28.4 (CH <sub>2</sub> )
11	32.1 (qC)	32.6 (qC)	31.9 (qC)	32.4 (qC)
12	80.7 (CH)	72.6 (CH)	74.3 (CH)	66.4 (CH)
13	98.2 (CH)	92.2 (CH)	98.2 (CH)	92.3 (CH)
14	30.6 (CH <sub>2</sub> )	27.4 (CH <sub>2</sub> )	30.7 (CH <sub>2</sub> )	31.2 (CH <sub>2</sub> )
15	34.2 (CH <sub>2</sub> )	29.3 (CH <sub>2</sub> )	35.9 (CH <sub>2</sub> )	27.6 (CH <sub>2</sub> )
16	69.1 (CH <sub>2</sub> )	69.6 (CH <sub>2</sub> )	62.2 (CH <sub>2</sub> )	62.9 (CH <sub>2</sub> )
17	32.0 (CH <sub>2</sub> )	32.0 (CH <sub>2</sub> )		
18	26.6 (CH <sub>2</sub> )	26.6 (CH <sub>2</sub> )		
19	27.2 (CH <sub>2</sub> )	27.2 (CH <sub>2</sub> )		
20	34.2 (CH <sub>2</sub> )	34.2 (CH <sub>2</sub> )		
21	62.4 (CH <sub>2</sub> )	62.4 (CH <sub>2</sub> )		

<sup>a</sup> Recorded at 294 K.<sup>b</sup> Recorded at 300 K.

The 2D structure of **1** was confirmed by 2D NMR (<sup>1</sup>H–<sup>1</sup>H COSY, HSQC, and HMBC) spectrums. Related to the downfield NMR signals, four <sup>1</sup>H–<sup>1</sup>H spin fragments were figured out: H<sub>2</sub>-2/H<sub>2</sub>-3, H-5/H-6/H-7/H-12, H-13/H<sub>2</sub>-14, and H<sub>2</sub>-21/H<sub>2</sub>-20 (Fig. 2). The location of CH<sub>2</sub>-4 was elucidated by HMBC correlations from H<sub>2</sub>-2 ( $\delta_{\text{H}}$  2.70, m; 1.67, m) to C-4 ( $\delta_{\text{C}}$  30.4), and H<sub>b</sub>-4 ( $\delta_{\text{H}}$  0.84, m) to C-5 ( $\delta_{\text{C}}$  37.2) and C-6 ( $\delta_{\text{C}}$  70.3) (Fig. 2). Then the linkage of rings A and B through C-6 and N-1 was suggested by HMBC correlations from H-6 ( $\delta_{\text{H}}$  1.74, m) to C-2 ( $\delta_{\text{C}}$  57.1), C-12 ( $\delta_{\text{C}}$  80.7), and C-16 ( $\delta_{\text{C}}$  69.1). The existence of ring C and hemiacetal group was

**Table 2**  
<sup>1</sup>H NMR data for **1–4** Recorded in pyridine-*d*<sub>5</sub> at 600 MHz, assigned based on HSQC.

No.	<b>1</b> <sup>a</sup>	<b>2</b> <sup>a</sup>	<b>3</b> <sup>b</sup>	<b>4</b> <sup>b</sup>
2	2.70 (m) 1.67 (m)	2.70 (m) 1.67 (m)	2.79 (m) 2.41 (m)	2.79 (m) 2.41 (m)
3	1.53 (m) 1.26 (m)	1.53 (m) 1.26 (m)	1.66 (m) 1.29 (m)	1.66 (m) 1.29 (m)
4	1.76 (m) 0.84 (m)	1.76 (m) 0.84 (m)	1.61 (m) 1.23 (m)	1.58 (m) 1.23 (m)
5	1.53 (m)	1.53 (m)	1.60 (m) 1.23 (m)	1.60 (m) 1.23 (m)
6	1.74 (m)	1.79 (m)	2.50 (m)	2.53 (m)
7	2.16 (br s)	2.06 (br s)	1.84 (m)	1.71 (m)
8	2.04 (m)	1.99 (m)	2.29 (m)	2.29 (m)
9	1.62 (m)	1.62 (m)	1.50 (m)	1.50 (m)
10	2.73 (m) 1.48 (m) 2.24 (m)	2.78 (m) 1.54 (m) 2.28 (m)	2.10 (m) 1.35 (m) 2.24 (m)	2.10 (m) 1.35 (m) 2.24 (m)
12	3.20 (d, 3.0 Hz)	4.20 (d, 2.4 Hz)	3.88 (m)	4.73 (d, 4.2 Hz)
13	5.14 (m)	5.75 (d, 2.4 Hz)	5.20 (dd, 9.6, 2.4 Hz)	5.70 (d, 3.0 Hz)
14	2.02 (m) 1.88 (m)	2.09 (m) 1.78 (m)	1.99 (m) 1.87 (ddt, 13.2, 4.8, 2.4 Hz)	2.08 (m) 1.22 (m)
15	1.25 (m)	1.88 (m)	1.56 (m)	2.07 (m)
16	2.59 (m) 1.80 (m)	1.10 (dd, 12.6, 4.2 Hz) 2.59 (m) 1.98 (m)	1.40 (m) 2.66 (d, 11.4 Hz) 2.38 (d, 11.4 Hz)	1.78 (m) 2.74 (d, 11.4 Hz) 2.38 (d, 11.4 Hz)
17	1.41 (m) 1.00 (m)	1.41 (m) 1.00 (m)		
18	1.41 (m)	1.41 (m)		
19	1.78 (m)	1.78 (m)		
20	1.77 (m)	1.77 (m)		
21	3.90 (dd, 14.4, 6.8 Hz)	3.90 (dd, 14.4, 6.8 Hz)		

<sup>a</sup> Recorded at 300 K.<sup>b</sup> Recorded at 313 K.**Fig. 1.** Structures of **1–4**.**Fig. 2.** <sup>1</sup>H–<sup>1</sup>H COSY and Key HMBC correlations of **1**.

revealed by HMBC correlations from H-12 ( $\delta_{\text{H}}$  3.20, d, 3.0 Hz) to C-13 ( $\delta_{\text{C}}$  98.2), H<sub>2</sub>-15 ( $\delta_{\text{H}}$  1.25, m) to C-12 and C-13. Finally, the bridge ring over CH-7 and qC-11 can be elucidated by HMBC correlations from H-7 ( $\delta_{\text{H}}$  2.16, br s) to C-8 ( $\delta_{\text{C}}$  20.7), as well as H-12 to C-8 and C-10 ( $\delta_{\text{C}}$  29.5). Thus a C<sub>20</sub> planar fragment harboring COHQ moiety of **1** was elucidated as in myrifabral A, whose structure was confirmed by single crystal X-ray analysis.<sup>8</sup>

The rest five carbon atoms in structure of **1** all showed ‘–CH<sub>2</sub>–’ signals in DEPT135 spectrum indicating that this C<sub>5</sub> moiety to be a

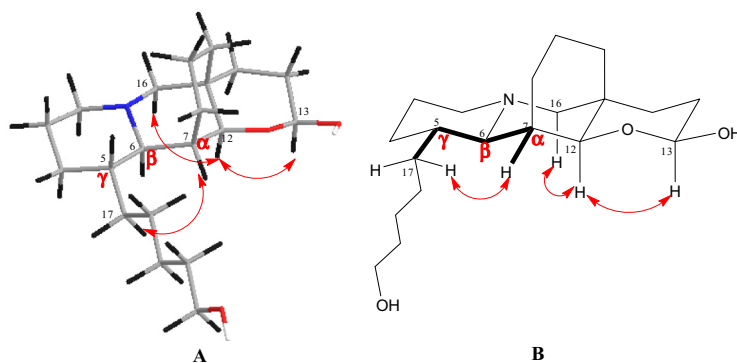


**Figure 3.** Key ROESY correlations of **1**. (A) showed in 3D sticks mode; (B) showed in Haworth mode (Bolded bonds marked the  $\gamma$ -gauche effect structure).

'-(CH<sub>2</sub>)<sub>5</sub>'. One of these methylenes (CH<sub>2</sub>-21,  $\delta_C$  62.4;  $\delta_H$  3.90, dd, 14.4, 6.8 Hz) was oxygenated, and that '-(CH<sub>2</sub>)<sub>5</sub>' was recognized as a *n*-pentanol group as in schoberine B.<sup>10</sup> Compared with C-5 in myrifabral A ('-CH<sub>2</sub>-',  $\delta_C$  30.6), C-5 in **1** ('-CH-',  $\delta_C$  37.2) indicated that *n*-pentanol group was directly bonded to C-5, which can be supported by HMBC correlations from H-17b ( $\delta_H$  1.00, m) to C-5. As a result, the 2D structure of **1** was established as shown in Fig. 2.

The relative configuration of **1** was resolved by its ROESY data and substituent effects. The NOE correlations of H-16a ( $\delta_H$  2.59, m)/H-12/H-13 ( $\delta_H$  5.14, m) revealed these protons are co-facial (deemed as  $\alpha$ -oriented), which required the bridge ring to be  $\beta$ -oriented (Fig. 3). According to the  $\beta$ -oriented bridge ring, the orientation of H-7 can be elucidated as  $\alpha$ . The fluctuations of NMR data of C-3, C-4, C-5, C-6, and C-7 compared with that of myrifabral A were probably resulted from the substituent on C-5. Among them,  $\delta_{C-7}$  in **1** was 5.1 ppm to lower frequency compared to that of  $\delta_{C-7}$  in myrifabral A, which suggesting the  $\gamma$ -gauche effect<sup>21</sup> caused by co-facial H-7 and *n*-pentanol group (Fig. 3B) and indicating the  $\alpha$ -oriented *n*-pentanol group. The 5 $\alpha$  configuration can also be supported by NOE correlation between H-7 and H-17b ( $\delta_H$  1.00, m). The <sup>1</sup>H and <sup>13</sup>C NMR data (Tables 1 and 2) of other positions on COHQ core matched well with that of myrifabral A suggesting that rings A and B on **1** possessed the same *trans* relationship as in myrifabral A, required the  $\alpha$ -oriented H-6. Thus the relative configuration of **1** was elucidated as 5 $\alpha$ , 6 $\alpha$ , 7 $\alpha$ , 12 $\alpha$ , and 13 $\alpha$ .

Accordingly, the structure of **2** was elucidated as the 13-epimer of **1** (Fig. 1). The NMR data of **1** and **2** can be distinguished by

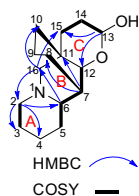


**Figure 4.** <sup>1</sup>H-<sup>1</sup>H COSY and Key HMBC correlations of **3**.

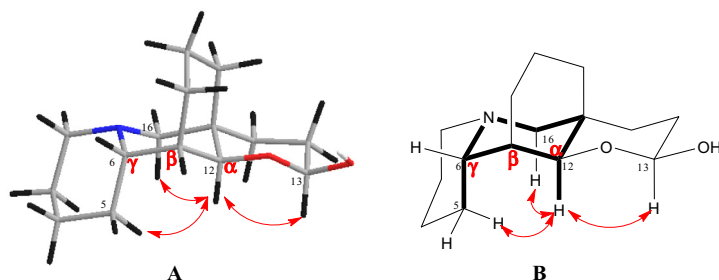


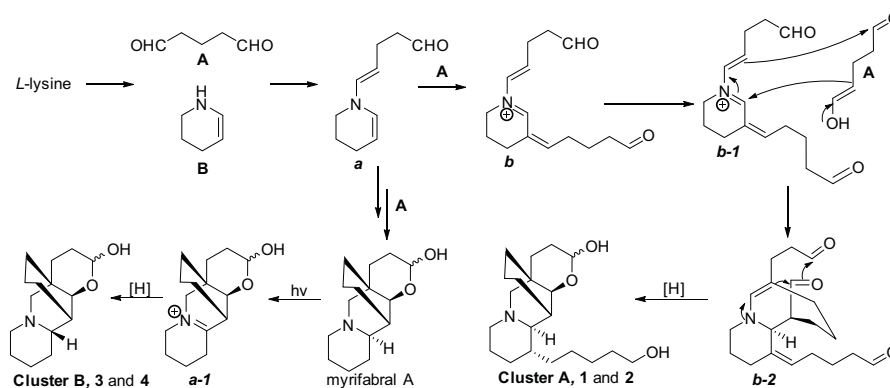
**Figure 5.** Key ROESY correlations of **3**. (A) showed in 3D sticks mode; (B) showed in Haworth mode (Bolded bonds marked the  $\gamma$ -gauche effect structure).

ROESY correlation between H-12 and H-13 (detected in **1**, negative in **2**) (S1.6 in Supporting Information). The population ratio of **1**:**2** as 1:0.66 in pyridine-*d*<sub>5</sub> was calculated by <sup>1</sup>H NMR spectrum integrals.

Cluster B (**3** and **4**)<sup>20</sup> was obtained as amorphous powder. Their molecular formula was established as C<sub>15</sub>H<sub>25</sub>NO<sub>2</sub> (identical to myrifabral A) by HRESIMS spectrum (*m/z* 252.1957 [M+H]<sup>+</sup>, calcd. for C<sub>15</sub>H<sub>26</sub>NO<sub>2</sub>, 252.1958), corresponding to four devices of hydrogen deficiency. The <sup>13</sup>C and DEPT NMR spectra of **3** and **4** presented 30 resonance signals comprising 2 × (10 × CH<sub>2</sub>, 4 × CH, and 1 × qC) carbon atoms (Fig. 1). In which the downfield '-CH-' signals ( $\delta_{C-13}$  = 98.2 in **3**;  $\delta_{C-13}$  = 92.3 in **4**) (Table 1) matched the double-oxygenated methenyl in hemiacetal epimers. The above mentioned data highly resembled to that of myrifabral A despite their NMR data differs at some positions, (Tables 1 and 2) which suggests **3** and **4** to be isomers of myrifabral A.

To unveil the 2D structure of **3**, its 2D NMR (<sup>1</sup>H-<sup>1</sup>H COSY, HSQC, and HMBC) spectrums were analyzed. Similar to **1**, four <sup>1</sup>H-<sup>1</sup>H spin fragments: H<sub>2</sub>-2/H<sub>2</sub>-3, H-5/H-6/H-7/H-12, H-13/H<sub>2</sub>-14, and H<sub>2</sub>-21/H<sub>2</sub>-20 can be figured out (Fig. 4). HMBC correlations from H-2 ( $\delta_H$  2.79, m; 2.41, m) to C-6 ( $\delta_C$  64.1), H-6 ( $\delta_H$  2.50, m) to C-16 ( $\delta_C$  62.2), and H-16a ( $\delta_H$  2.66, d, 11.4 Hz) to C-2 ( $\delta_C$  54.8) suggests rings A and B were linked by N-1 and C-6 (Fig. 4). Existence of ring C can be supported by HMBC correlations from H-16a to C-15 ( $\delta_C$  35.9), H-7 ( $\delta_H$  1.84, m) to C-11 ( $\delta_C$  31.9), and H-13 ( $\delta_H$  5.20, dd, 9.6, 2.4 Hz) to C-12 ( $\delta_C$  74.3) and C-15 ( $\delta_C$  35.9). The bridge ring over CH-7 and qC-11 was supported by HMBC correlations from H-16a to C-10 ( $\delta_C$  29.2), and H-7 to C-8 ( $\delta_C$  19.2). Consequently, the 2D structure of **3** was elucidated as the same as myrifabral A (Fig. 4).

The relative configuration of **3** was elucidated by its ROESY spectrum and substituent effects. The NOE correlations of H-16a/H-12 ( $\delta_H$  3.88, m)/H-13 were detected as in the case of **1**, which indicating  $\beta$ -oriented bridge ring and  $\alpha$ -oriented H-7, H-12, and H-13 (Fig. 5). The <sup>13</sup>C NMR data of **3** (Table 1) mainly differed from myrifabral A at C-2 ( $\Delta\delta_C$  -2.4), C-4 ( $\Delta\delta_C$  -4.2), C-6 ( $\Delta\delta_C$  -2.3), C-9 ( $\Delta\delta_C$  +4.1), and C-12 ( $\Delta\delta_C$  -6.3), and we deduced



Scheme 1. Hypothesized biogenetical pathway of 1–4.

that it was resulted from their opposite H-6 orientation. The  $\beta$ -oriented H-6 could be supported by: 1) the lower frequency shifted  $\delta_{C-12}$  ( $\Delta\delta_C -6.3$ ) caused by  $\gamma$ -gauche effect<sup>21</sup> between axial bond of C<sub>6</sub>-C<sub>5</sub> and H-12 of **3** (Fig. 4B); 2) the NOE correlation of H-5a ( $\delta_H$  1.60, m)/H-12 ( $\delta_H$  4.73, d, 4.2 Hz) of **4**. As a result, the relative configuration of **3** was elucidated as 5 $\alpha$ , 6 $\beta$ , 7 $\alpha$ , 12 $\alpha$ , and 13 $\alpha$ . By the same manner, the structure of **4** was elucidated as the 13-epimer of **3** (Fig. 1). The ROESY spectra of **3** and **4** showed difference at the NOE correlation spot between H-12 and H-13 (detected in **3**, negative in **4**) (S2.6 in Supporting Information).

Previously reported  $\beta$ -myrifabral A and  $\alpha$ -myrifabral A were proved to be two pairs of enantiomers by chiral column analysis on HPLC after chemical modification.<sup>8</sup> Cluster A (**1** and **2**) and cluster B (**3** and **4**) were directly subjected to four different types of chiral column analysis on HPLC, but there was no evidence supported they are enantiomers. Alkaloids **1** and **2** were evaluated against hepatitis C virus (HCV) in vitro as previously reported method,<sup>8,9</sup> and showed moderate inhibition activity against hepatitis C virus (HCV) replication with therapeutic index ( $CC_{50}/EC_{50}$ ) of 74.0 (VX-950 as a positive control).

A hypothesized biogenetical pathway of **1–4** starting from L-lysine similar to myrifabral A and B was suggested (Scheme 1). Reactive C<sub>5</sub> units **A** and **B** could be derived from L-lysine.<sup>4</sup> Condensation of **A** and **B** then yield intermediate **a**, which could incorporate unit A to afford myrifabral A as previously suggested pathway. Then an imine intermediate **a-1** could be resulted from ultraviolet radiation,<sup>22</sup> and further reduced to cluster B. On pathway to cluster A, the C-15 intermediate **b-1** could be achieved from **a**, and condensed with one unit A to establish **b-2**. Consequently, cluster A could be achieved from **b-2** through condensation and reduction procedures.<sup>8</sup>

## Acknowledgment

This research was supported financially by the National Natural Science Foundation of China (No. 21372228 and 31500035).

## A. Supplementary data

Supplementary data (1D and 2D NMR, ESIMS, and HRESIMS spectra for **1–4**) associated with this article can be found, in the online version, at <http://dx.doi.org/10.1016/j.tetlet.2016.11.001>. These data include MOL files and InChIKeys of the most important compounds described in this article.

## References

- Pham VC, Jossang A, Chiaroni A, Sévenet T, Bodo B. *Tetrahedron Lett.* 2002;43:7565–7568.
- Pham VC, Jossang A, Grellier P, et al. *J Org Chem.* 2008;73:7565–7573.
- Gravel E, Poupon E. *Nat Prod Rep.* 2010;27:1630–1680.
- Erwan P, Edmond G. *Chem Eur J.* 2015;21:10604–10615.
- Pham VC, Jossang A, Sévenet T, Nguyen VH, Bodo B. *Eur J Org Chem.* 2009;74:1412–1416.
- Pham VC, Jossang A, Sévenet T, Nguyen VH, Bodo B. *Tetrahedron.* 2007;63:11244–11249.
- Cao MM, Huang SD, Di YT, et al. *Org Lett.* 2014;16:528–531.
- Cao MM, Zhang Y, Li XH, et al. *J Org Chem.* 2014;79:7945–7950.
- Cao MM, Zhang Y, Huang SD, et al. *J Nat Prod.* 2015;78:2609–2616.
- Cao MM, Zhang Y, Peng ZG, Jiang JD, Gao YJ, Hao XJ. *RSC Adv.* 2016;6:10180–10184.
- Huang SD, Zhang Y, Cao MM, et al. *Org Lett.* 2013;15:590–593.
- Pham VC, Jossang A, Chiaroni A, Sévenet T, Nguyen VH, Bodo B. *Org Lett.* 2007;9:3531–3534.
- Nocket AJ, Weinreb SM. *Angew Chem Int Ed.* 2014;53:14162–14165.
- Nocket AJ, Feng YQ, Weinreb SM. *J Org Chem.* 2015;80:1116–1129.
- Song DP, Wang ZS, Mei RM, et al. *Org Lett.* 2016;18:669–671.
- Cao MM, Zhang Y, Huang SD, Peng ZG, Jiang JD, Hao XJ. *Tetrahedron Lett.* 2016;57:4021–4023.
- Li XH, Zhang Y, Zhang JH, et al. *J Nat Prod.* 2016;79:1203–1207.
- Zhang JH, Guo JJ, Yuan YX, et al. *Fitoterapia.* 2016;112:217–221.
- Colorless gum;  $[\alpha]_D^{23} -27$  (c 0.3, MeOH); UV (MeOH)  $\lambda_{max}$  (log  $\epsilon$ ) 204 (2.81); <sup>1</sup>H and <sup>13</sup>C NMR data, see Tables 1 and 2; positive ESIMS  $m/z$  338, [M+H]<sup>+</sup>; positive HRESIMS  $m/z$  found 337.2635 for [M]<sup>+</sup>; calcd. for C<sub>20</sub>H<sub>35</sub>NO<sub>3</sub>, 337.2617 [M]<sup>+</sup>.
- Amorphous powder; <sup>1</sup>H and <sup>13</sup>C NMR data, see Tables 1 and 2; positive ESIMS  $m/z$  252 [M+H]<sup>+</sup>; positive HRESIMS  $m/z$  252.1957 [M+H]<sup>+</sup>, calcd. for C<sub>15</sub>H<sub>26</sub>NO<sub>2</sub>, 252.1958 [M+H]<sup>+</sup>.
- Barfield M, Yamamura SH. *J Am Chem Soc.* 1990;112:4747–4758.
- Ahmed SA, Khairou KS, Asghar BH, Muathen HA, Nahas NMA, Alshareef HF. *Tetrahedron Lett.* 2014;55:2190–2196.